Identification of forming limits at fracture using an in-plane biaxial tensile test with a dedicated cruciform specimen

Xiao Song, Lionel Leotoing, Dominique Guines, Eric Ragneau

Identification of forming limits at fracture using an in-plane biaxial tensile test with a dedicated cruciform specimen

X. SONG [a], L. LEOTOING [b], D. GUINES [c] and E. RAGNEAU [d]

Université Européenne de Bretagne, France
INSA-LGCGM-EA 3913, 20 Av. des Buttes de Coësmes, CS 70839, 35708 Rennes Cedex 7, France
[a] E-mail: xiao.song@insa-rennes.fr, [b] E-mail: lionel.leotoing@insa-rennes.fr,
[c] E-mail: dominique.guines@insa-rennes.fr and [d] E-mail: eric.ragneau@insa-rennes.fr

ABSTRACT. *Three shapes of cruciform specimen from literatures are redesigned and their efficiencies for identifying the forming limits at fracture are considered by means of finite element numerical investigations. Based on the numerical investigation, a dedicated shape of cruciform specimen is proposed. The AA5086 and DP600 sheets with a thickness of 2mm are adopted in the in-plane biaxial tensile tests. The digital image correlation (DIC) is used to calculate the deformation field on the specimen surface. A method based on the evolution of major strain and the observation of the macroscopic image of specimen surface is proposed to identify the onset of fracture and the limit strains at fracture.*

INTRODUCTION

Necking can cause undesirable surface defects in sheet metal components, so limits in sheet metal forming are generally controlled by localized necking rather than fracture. However, under certain conditions, fracture can precede necking in traditional sheet metal forming processes, particularly with loading under biaxial tension [1]. In that case, the limit strain by fracture rather than the limit strain by necking determines the deformation achievable. Moreover, it is demonstrated that neck formation is delayed or suppressed in some processes, like single point incremental forming (SPIF), and greater deformability can be achieved in parts manufactured by SPIF than by traditional sheet metal forming processes. The traditional forming limit curve (FLC) is inapplicable to describe failure, and the fracture forming limit line (FFL) should be employed [2, 3].

The in-plane biaxial tensile test with a dedicated cruciform specimen can be used to identify the forming limits at necking under linear paths [4] and non-linear paths [5], so it could be an interesting method to identify the forming limits at fracture. For investigation of fracture in biaxial tensile test, a dedicated cruciform specimen should be designed to ensure that the fracture occurs at the central point of the cruciform specimen. This condition permits to control the strain path of fracture area thanks to the displacement of the four actuators.

In this research, a dedicated cruciform specimen is proposed for investigating the fracture based on the comparison of three redesigned cruciform specimens. A method based on the evolution of major strain and the observation of the macroscopic image of specimen surface is proposed to identify the onset of fracture and the limit strains at fracture.

Cruciform specimen design

Redesign of three cruciform specimens

During biaxial tensile test for investigating the fracture, it is very hard to keep that the fracture appears in the central point without thickness reduction. However, if the final thickness of the central zone is too small, the reduced zone can not represent the original sheet in the thickness direction. Therefore, the final thickness of central zone should be designed as large as possible on condition that fracture will appear at the central point. In previous studies with the use of cruciform specimens, the maximum rate of the thickness value at the reduced zone to the original sheet thickness value reaches just 25%, and in most cruciform specimens the rate is even less than 10%. In this research, 2mm metallic sheets of AA5086 and DP600 are adopted, and the aim is to design a cruciform specimen with a thickness of 0.75mm at the central point of the reduced zone (37.5% of the original thickness value).

Three cruciform specimens reported in previous literatures are selected due to the observation of large strains in the central zone. As shown in Figure 1, the original sheet thickness, the thickness of reduced zone and the dimension of central zone of each cruciform specimen are redesigned. Through FE software ABAQUS, their efficiencies for investigation of fracture under equi-biaxial tension are numerically investigated.

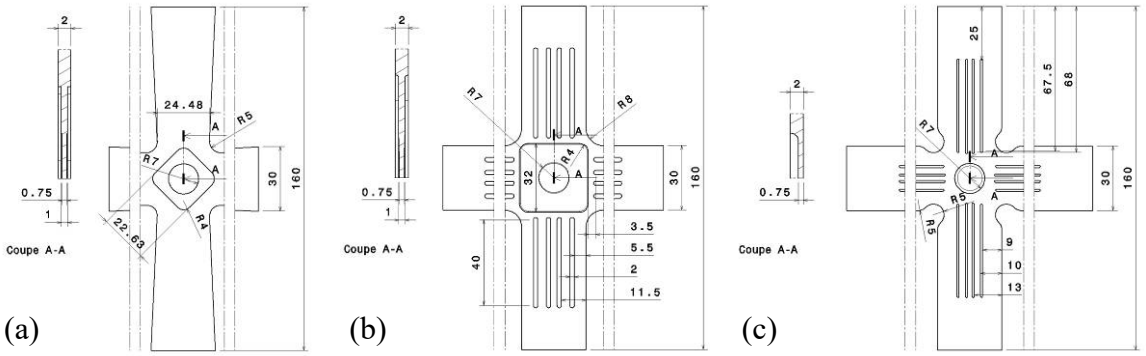

Figure 1. Geometies of cruciform specimen: (a) specimen 1, (b) specimen 2, (c) specimen 3.

For the geometry of specimen 1 [6], two steps of thickness reduction are adopted. The shape of the first thickness reduction is a circle with flat bottom, while the shape of the second thickness reduction is a square with rounded corner and with edges rotated by 45° relative to the axes of the arms. Moreover, four tapered arms are used. For the geometry of specimen 2 [7], two steps of thickness reduction are used. The first thickness reduction is a circle with an arc profile in the thickness direction, and the second thickness reduction is a square and its edges are parallel to the arm. Four slits are

added at the arm. For the geometry of cruciform specimen 3 [8], one step of thickness reduction is used and the shape of thickness reduction is a circle with a flat bottom. Slits are arranged with different locations at each arm. Furthermore, for the specimen 1 and 2, the thickness of intermediate zone is 1mm.

Numerical investigation of the redesigned cruciform specimens

The equi-biaxial tensile test is simulated and only one-quarter of the specimen is analyzed for considering the symmetry of the specimen geometry. For elasticity, Young's modulus E=70GPa and Poisson's ratio v=0.33 are considered. For plasticity, isotropic Mises yield criterion and a representative isotropic hardening behaviour of AA5086 are adopted. For each specimen, the tetrahedral elements of type C3D4 are used and the mesh size at the central area is 0.25mm.

All the numerical results presented correspond to the moment when the maximum value of major strain reaches 20% at one point of the specimen. At the same time, the field of equivalent plastic strain and the evolution of strain along the specified path are presented.

Figure 2 shows the numerical results of specimen 1. The maximum value of major strain and the maximum value of equivalent plastic strain are all located at the transition zone of arms. From the evaluations of major strain and equivalent plastic strain along path 1, it can be seen that the major strain is much higher at the transition of arms (18%) than at the central point (6%). The equivalent plastic strain has two rapid changes at the boundary between two zones with different thicknesses.

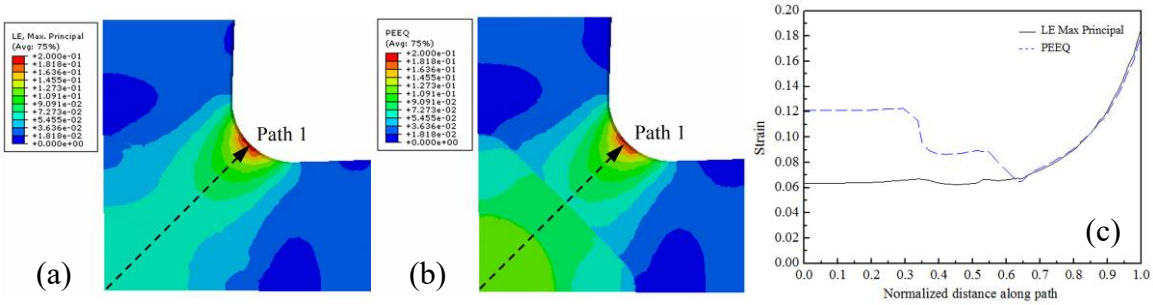

Figure 2. Numerical results of specimen 1: (a) Field of major strain, (b) Field of equivalent plastic strain, (c) Strains along path 1

Figure 3 shows the numerical results of specimen 2. The maximum value of major strain reaches 20% at the tip of slit while the maximum value of equivalent plastic strain is located at the central point. For path 1, the value of major strain is much higher at the slit (17%) than at the central point (7%). For path 2, there is a sharp increase at the boundary of the reduced zone and the value of major strain is about 19%, which may cause fracture.

Figure 4 shows the numerical results of specimen 3. The maximum value of major strain reaches 20% at the tip of slit and the maximum value of equivalent plastic strain is also located at the tip of slit. For path 1, the value of major strain is much higher at the slit (18%) than at the central point (7%). There is an increase in the major strain and equivalent plastic strain at the boundary of the reduced central zone because of the flat

bottom, where fracture may happen. Same phenomenon can be seen in path 2. Moreover, the concave shape of the transition zone of arms is complex.

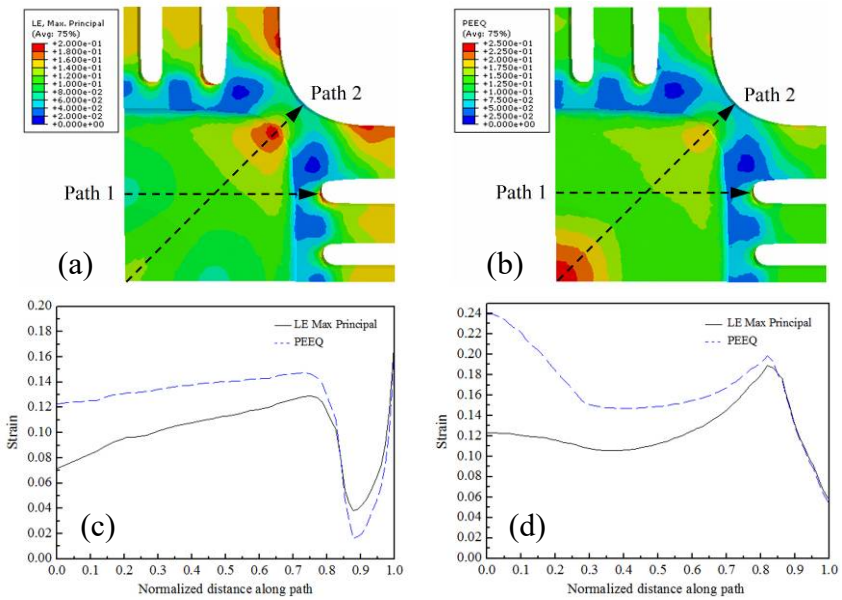

Figure 3. Numerical results of specimen 2: (a) Field of major strain, (b) Field of equivalent plastic strain, (c) Strains along path 1, (d) Strains along path 2.

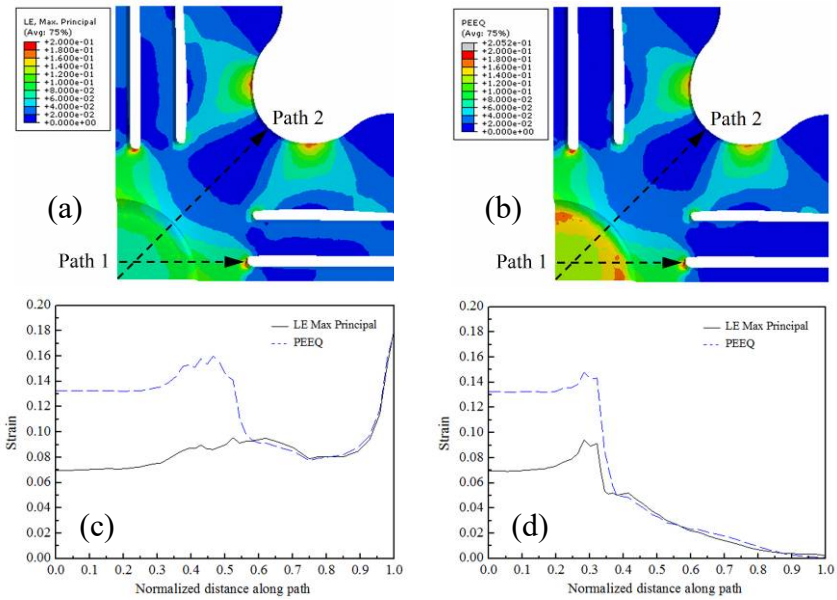

Figure 4. Numerical results of specimen 3: (a) Field of major strain, (b) Field of equivalent plastic strain, (c) Strains along path 1, (d) Strains along path 2.

Based on the above results, a basic cruciform specimen including one step of thickness reduction, an arc profile in the thickness direction of a circular reduced zone and several slits at each arm is considered and the dimensions will be optimized.

An optimized cruciform specimen

An optimized cruciform specimen is proposed, as shown in Figure 5. A circle zone in the center of the specimen is reduced with a radius value of 7mm. In the thickness direction of the reduced zone, a circle profile is adopted to lead the strain localization to the central point. Six slits are added at each arm and the arrangement of slits is optimized.

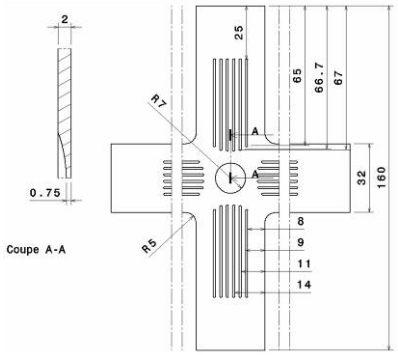

Figure 5 Geometry of the optimized cruciform specimen

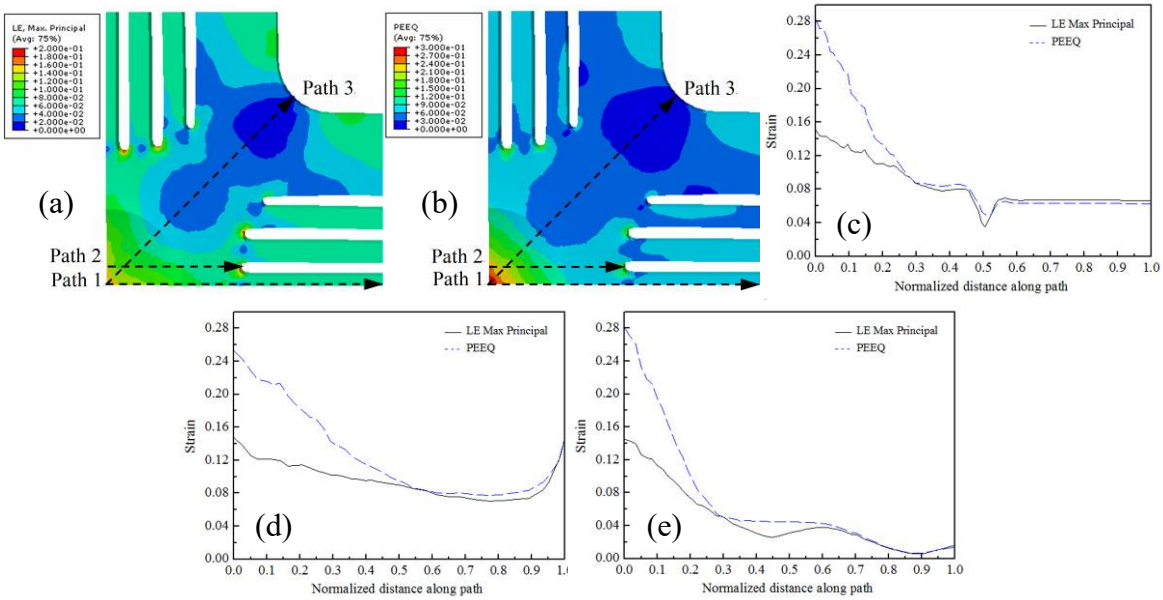

Figure 6. Numerical results of the optimized cruciform specimen: (a) Field of major strain, (b) Field of equivalent plastic strain, (c) Strains along path 1, (d) Strains along path 2, (e) Strains along path 3.

Figure 6 shows the numerical results of the optimized specimen. The maximum value of major strain reaches 20% at the tip of slit, while the maximum value of equivalent plastic strain reaches about 30% at the central point. From the evaluations of major strain and equivalent plastic strain along path 1, path 2 and path 3, it can be seen that the values of major strain and equivalent plastic strain are much higher at the central point than at the arm or at the transition zone of arms. Though the value of major

strain is little higher at the slit than at the central point, the value of equivalent plastic strain is much higher at the central point than at the slit. Therefore, the optimized cruciform specimen has potential to obtain fracture at the central point.

Experimental validation

Biaxial testing machine and strain measurement

As shown in Figure 7, the experimental device is a servo-hydraulic testing machine provided with four independent dynamic actuators allowing biaxial tensile tests on cruciform specimens following two perpendicular axes. The central area of the cruciform specimen can be deformed under various strain paths when different speeds are set on the two perpendicular axes. Here, the speed of 1mm/s is used for two perpendicular axes to produce the equi-biaxial tension state.

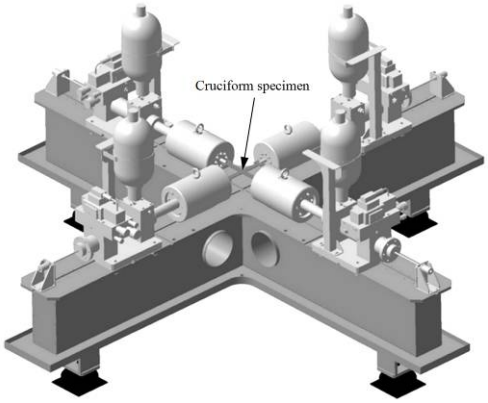

Figure 7. The in-plane biaxial tensile machine

The digital image correlation (DIC) is used to evaluate the strain components during the tests. A Fastcam APX-RS camera associated with a macro lens is used to capture the consecutive images and an acquisition of 250 i/s is adopted. The commercial digital imaging program CORRELA2006, developed by LMS at the University of Poitiers, is employed to evaluate the surface strains of the cruciform specimen. The DIC technique requires a random speckle pattern so that the image of the surface of specimen could be represented by a discrete function of values depending on grey levels. However, the surface of the reduced side of the cruciform specimen is curved while the surface of the non-reduced side is plane. The measuring results of strains by the two shapes of surface will be compared.

Identification of the forming limits at fracture

Figure 8 shows the surface images (reduced side) of the AA5086 specimen under biaxial tension and the evolution of strain. It can be seen that the fracture occurs at the central point. The central zone with the size of 2.5×2.5mm is used to measure the evolution of major strain. The level of major strain in the central zone increases with the time and a macrosopic crack occurs accompanying with an abrupt change of major strain during 0.004s at the last of test, while there is no macrosopic crack before. The

major strain and the minor strain at 0.004s before fracture can be defined as the forming limit strains at fracture. The identified major strain at fracture by the surface of the reduced side is about 0.324.

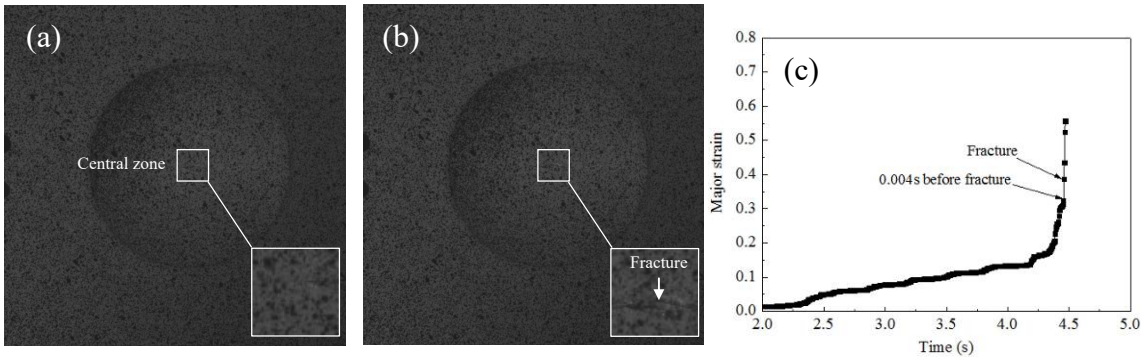

Figure 8. Identification of fracture for AA5086 specimen (reduced side) under biaxial tension: (a) 0.004s before fracture, (b) fracture, (c) Evolution of strain.

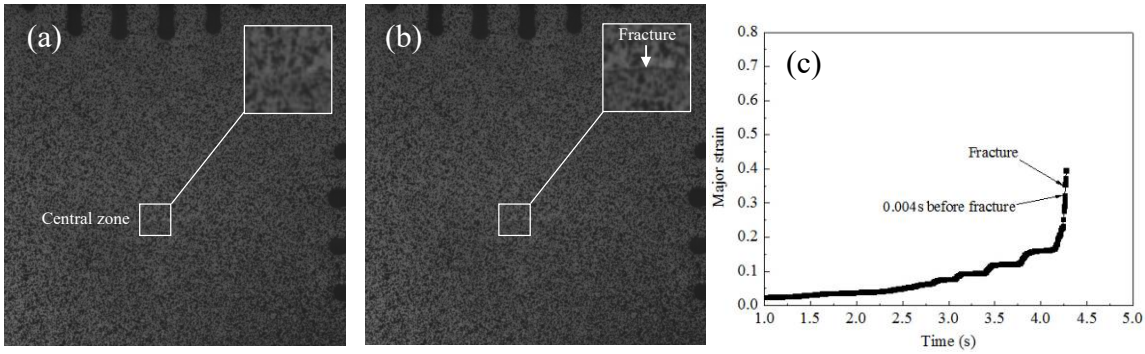

Figure 9. Identification of fracture for AA5086 specimen (non-reduced side) under biaxial tension: (a) 0.004s before fracture, (b) fracture, (c) Evolution of strain.

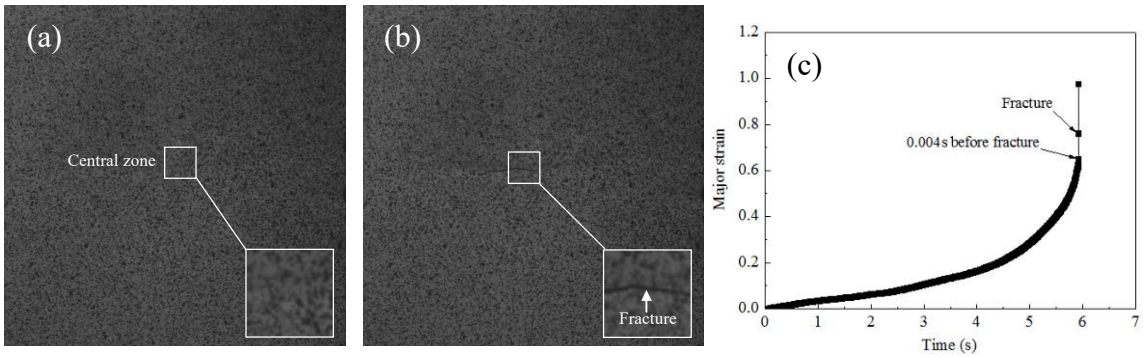

Figure 10. Identification of fracture for DP600 specimen (non-reduced side) under biaxial tension: (a) 0.004s before fracture, (b) fracture, (c) evolution of strain.

Figure 9 shows the identification result of fracture by the non-reduced side of the AA5086 specimen under biaxial tension. The fracture in the center of the cruciform specimen can also be identified by the evolution of major strain and the observation of macroscopic images of specimen surface at the non-reduced side. The identified major

strain at fracture by the surface of the non-reduced side is about 0.321, which is almost the same to the value identified by the surface of the reduced side. It means that the effect of the surface shape of the proposed cruciform specimen is very small.

The shape of the optimized cruciform specimen is also used for investigating the forming limits of DP600 sheets under equi-biaxial tension. As shown in Figure 10, the fracture happens at the central point of the cruciform specimen and the onset of the fracture can also be identified by the evolution of major strain and the observation of the macroscopic images of specimen surface. The identified major strain at fracture by the surface of the non-reduced side is about 0.650

CONCLUSIONS AND PERSPECTIVES

For the proposed shape of cruciform specimen, experiments have been led on 2mm metallic sheets of AA5086 and DP600. Results show that fracture happens at the central point of the cruciform specimen, which is in good agreement with the numerical simulation result. The onset of fracture and the limit strains at fracture for the metallic sheets of AA5086 and DP600 can be identified by the proposed method based on the evolution of major strain and the observation of the macroscopic image of specimen surface, due to the fact that the appearance of macroscopic crack is accompanied with an abrupt increase of major strain.

In the next study, the forming limit strains at fracture under different linear strain paths will be identified by the proposed method with the optimized cruciform specimen. Moreover, different ductile fracture criteria for determining the forming limit strains at fracture will be calibrated in numerical simulations.

REFERENCES

1. Bruschi, S., Altan, T., Banabic, D., Bariani, P.F., Brosius, A., Cao, j., Ghiotti, A., Khraisheh, M., Merklein, M. and Tekkaya, A.E. (2014) CIRP Ann. Manuf. Techn. 63, 727-749.
2. Silva, M.B., Nielsen, P.S., Bay, N. and Martines, P.A.F. (2011) Int. J. Adv. Manuf. Tech. 56, 893-903.
3. Isik, K., Silva, M.B., Tekkaya, A.E. and Martines, P.A.F. (2014) J. Mater. Process. Tech. 214, 1557-1565.
4. Léotoing, L., Guines, D., Zidane, I. and Ragneau, E. (2013) J. Mater. Process. Tech. 213, 856-863.
5. Léotoing, L. and Guines, D. (2015) Int. J. Mech. Sci. 99, 21-28.
6. Lee, R. S. and Chien, T. W. (2015) Key. Eng. Mat. 626, 275-280.
7. Zidane, I., Guines, D., Léotoing, L. and Ragneau, E. (2010) Meas. Sci. Technol. 21, 055701(11pp).
8. Liu, W., Guines, D., Léotoing, L. and Ragneau, E. (2015) Int. J. Mech. Sci. 101, 387-398.